Cifuentes-Cabezas, MS.; Galinha, C.; Crespo, J.; Vincent Vela, MC.; Mendoza Roca, JA.; Alvarez Blanco, S. (2023). Nanofiltration of wastewaters from olive oil production: Study of operating conditions and analysis of fouling by 2D fluorescence and FTIR spectroscopy. Chemical Engineering Journal. 454 (1)(1385-8947). https://doi.org/10.1016/j.cej.2022.140025

Nanofiltration of wastewaters from olive oil production: study of operating conditions and analysis of fouling by 2D fluorescence and FTIR spectroscopy

Magdalena Cifuentes-Cabezas[a*], Claudia F. Galinha[b], João G. Crespo[b], María Cinta Vincent-Vela[a,c], José Antonio Mendoza-Roca[a,c], Silvia Álvarez-Blanco[a,c]

[a] Research Institute for Industrial, Radiophysical and Environmental Safety (ISIRYM), Universitat Politècnica de València, C/Camino de Vera s/n, 46022, Valencia, Spain

[b] LAQV-REQUI*M*TE, Chemistry Department, NOVA School of Science and Technology, Universidade NOVA de Lisboa, 2829-516 Caparica, Portugal

[c] Department of Chemical and Nuclear Engineering, Universitat Politècnica de València, C/Camino de Vera s/n, 46022, Valencia, Spain

*magcica@posgrado.upv.es

Abstract

The presented work tries to solve the problem of the large volumes of oil mill wastewater (OMW). For this, nanofiltration is presented as a possible second stage of treatment. Different membranes were tested under different operating conditions, varying cross flow velocity (CFV) and transmembrane pressure (TMP), in order to obtain a concentrate rich in phenolic compounds and also an adequate permeate able to be returned to the process as machinery cleaning water. The NF270 membrane under the conditions of 1 ms^{-1} CFV and 10 bar of TMP was observed to be the best to concentrate the phenolic compounds, with high permeate flux and low fouling. Different types of tests were performed: membrane adsorption tests with different compounds, nanofiltration tests with a model solution (MS) to analyse fouling and check the effectiveness of the cleaning protocol and, finally, the selected NF270 membrane was tested with OMW. Also, for the first time, 2D fluorescence spectroscopy and Fourier-transform infrared spectroscopy (FTIR) were used together as tools to study membrane fouling. From the adsorption tests it was observed that all the considered compounds had an effect on the membrane surfaces, which was also confirmed from the nanofiltration tests (with the DM900 membrane the most affected). After cleaning, the membranes fouled with MS and OMW did not recover the spectra of the pristine membranes but, instead, matched the spectra presented by the new membranes subjected to the cleaning protocol. Finally, the following a suitable membrane for this purpose is selected In addition, it has been proved that the used spectroscopic techniques are a feasible option for the study of both fouling and efficiency of cleaning protocols.

Keywords

Olive mill wastewater; Phenolic compounds; Nanofiltration (NF); 2D fluorescence spectroscopy; Fourier-transform infrared spectroscopy (FTIR)

1. Introduction

As the world's population continues to grow and social pressures and awareness of the need for environmental improvement increase, solutions to environmental issues of industry must be found. One of the greatest problems is the large amount of wastewater generated each year by various industrial sectors. One of these sectors, which mainly affects Mediterranean countries, is the olive oil industry, where olive mill wastewater (OMW) is enormously produced. This wastewater has a high content of organic matter, an acidic profile and a large quantity of phytotoxic compounds. These phytotoxic compounds in OMW are phenolic compounds, which are, at the same time, harmful to the environment, but they also show an outstanding antioxidant activity, making them potentially valuable for commercialization [1]. Different processes have been proposed and developed for the treatment of OMW, including membrane processes. These processes are basically a separation generated by a membrane. This membrane acts as a semi-permeable barrier that separates two phases by selectively restricting the movement of components through it. This separation occurs through different driving forces, being pressure-driven separation the most widely applied in wastewater treatment [2]. The advantages of membrane technologies, such as modularity, compactness, easy scalability and adaptability to different capacities make them a promising alternative in situations where wastewater treatment is combined with the recovery of useful components [3]. Within these membrane processes, nanofiltration (NF) is a widely used process for the treatment of OMW. Due to its high capacity to retain a large amount of organic content as well as monovalent (partially) and divalent ions, it produces a high quality final permeate (with low organic matter concentration and ionic content) suitable for reuse in irrigation, and a concentrate enriched in phenolic compounds [4].

Today there are still some problems in upscaling some membrane process to treat industrial wastewaters due to fouling. The complexity of fouling is due to the presence of multiple species that can interact with each other to form dense and compact fouling layers through pore blockage, adsorption and/or cake formation [5]. This fouling shortens the life of the membranes due to the increase frequency of cleaning procedures. Membrane fouling increases wastewater treatment costs and energy consumption, which affects the industrial application of membranes [6]. Therefore, it is recommended to integrate pre-treatment processes to mitigate fouling phenomena. The combination of different techniques and sequential membrane processes has proven to be a good approach to prevent membranes from fouling [7–9]. Paraskeva et al. [10] and Coskun et al. [11] investigated different membrane techniques for the treatment of OMW. These authors were able to reduce total chemical oxygen demand (COD) with the combination of ultrafiltration (UF), NF and reverse osmosis (RO). Sanches et al. [12] studied the treatment of OMW by a sequence of dissolved air flotation pre-treatment and NF at pilot plant scale, reaching a reduction between 83 to >99% of suspended solids and 53 to 77% of COD. Furthermore, in previous studies by the authors of this work [13] a permeate highly enriched in phenolic compounds was obtained by

means of UF with organic membranes. However, this stream was very diluted. Therefore, this permeate could be later concentrated by techniques such as NF. The utilization of integrated membrane processes to obtain a concentrated stream enriched in phenolic compounds has also been proposed by other authors [14]. However, the main limit of OMW treatment by membrane processes is the total cost involved (5-10 €·m^{-3}) [15]. These costs, which are associated with electricity, technical issues and chemical are directly related to the main disadvantage of membrane technologies, which is membrane fouling. Fouling raises the cost of electricity, as well as the dose of chemicals used in membrane cleaning. This is the reason why this work is focused on membrane fouling. The main advantage of the proposed method, as reported by Kamali et al. [16], is its potential to be a "zero" waste process through valorization of secondary concentrate streams.

The environmental impact of the proposed OMW treatment is also a critical issue. Membrane processes do not require the addition of chemicals. Thus, they generate streams that are concentrated in phenolic compounds, whose recovery can cover the initial costs of the process, and high-quality water that can be reused as machine washing water. All this makes treatment of OMW with membranes potentially possible and sustainable from an environmental point of view. On the other hand, establishing appropriate operating conditions and studying the interaction between the membrane and the compounds present in the influent allows a better understanding of the system, control fouling and thus improve membrane performance [17]. Therefore, understanding the fouling mechanism of individual foulants is crucial for fouling prevention and control in order to find hindrance strategies and optimise cleaning treatments.

The lack of papers about characterization of fouling components in NF membranes after the treatment of OMW, has generated the need to search for techniques that deliver fast and complete results. To date, various methods have been proposed and/or applied to characterise fouling, such as scanning electron microscopy with energy dispersive X-ray spectroscopy, atomic force microscopy, three-dimensional (3D) optical coherence tomography, molecular spectroscopic methods and others [18,19]. Spectroscopic techniques rely on the interaction of electromagnetic radiation with the sample, where the radiation can be absorbed, transmitted or scattered. These techniques have several advantages, such as low sample consumption, rapid analysis that does not require pre-treatment of the samples, as well as ease of use, reduction in the use of solvents, minimising potential environmental impact and providing a wealth of information in a short time [18,20].

In 2D fluorescence spectroscopy, the natural fluorescence of a variety of compounds is used for their detection. When a fluorophore compound is excited, it emits light that can be recorded by fluorescence spectroscopy. The spectra generated can provide quick and useful information about the composition of the samples, with the help of mathematical tools. This technique has been used in various fields such as reverse electrodialysis [21], membrane bioreactors [22] and in the food

industry [23,24]. An outstanding advantage of 2D fluorescence spectroscopy is that it can be used for in in situ monitoring of fouling. Although the number of papers on this matter is very limited, the results obtained were promising. Therefore, this work could provide the first indications to check if this technique is appropriate to characterize OMW-fouled NF membranes prior to further studies to implement this technique for in situ characterization. Fourier transform infrared spectroscopy (FTIR) is another method often used to characterise membrane materials and impurities. In this case, the spectra profiles comprise specific bond stretchs and allow the identification of the chemical species in the sample [25].

The results are also readily available and can provide valuable information on the composition. Principal component analysis (PCA) and partial least squares (PLS) are some of the multivariate techniques commonly used to deconvolute and interpret spectroscopic data [26].

In this paper, NF was analysed as a possible second stage treatment after UF, for the recovery of phenolic compounds from an olive oil washing wastewater (OOWW). The NF process was fed with the permeate obtained from a previous UF step that demonstrated to be efficient to remove a large amount of the organic matter and obtain a permeate rich in phenolic compounds [13]. Different NF membranes and operating conditions were tested to obtain a concentrated stream containing phenolic compounds and a permeate stream suitable to be recycled to the process as machinery wash water. The membranes used in this study are commercial. Although good results have been reported with modified membranes, most membrane manufacturing and modification strategies are not yet implemented at industrial scale due to cost and repeatability problems [27]. Moreover, the utilization of 2D fluorescence spectroscopy and FTIR as tools to investigate membrane fouling was considered. Finally, a PCA data analysis was employed to evaluate the efficiency of the cleaning protocols using the data obtained from these techniques. The purpose of this study was, firstly, to find the best membrane and operating conditions for the recovery of these antioxidants with NF and, secondly, to investigate the potential of these spectroscopic techniques to study the fouling phenomenon and cleaning protocols of the membranes.

2. Materials and Methods

2.1 Nanofiltration experiments for process optimization

2.1.1 Nanofiltration process

Four polymeric membranes with different properties were analysed as a second stage of treatment of an OOWW. All the membranes were first conditioned under the same protocol. The membranes were submerged for hydration for 24 hours in pure water (conductivity <40 µS/cm) and then compacted for three hours. The operating conditions were: transmembrane pressure (TMP) of 16 bar and a cross-flow velocity (CFV) of 1 $m \cdot s^{-1}$. The conditions used were based on studies carried out by Sanchez-Arévalo et al. [28] and following the standard procedures for membrane

compaction [29]. Once the compaction was finished, the hydraulic permeability (K) was measured and obtained using the following equation:

$$J = K \cdot \Delta P \quad \text{(Eq.1)}$$

Where J ($L \cdot h^{-1} \cdot m^{-2}$) is the permeate flux and ΔP (bar) the TMP. Previously, a UF process was carried out as first membrane process stage to eliminate the major organic matter. It was performed with an UP005 Microdyn-Nadir membrane, under the operating conditions of 2 bar of TMP and CFV of 2.5 $m \cdot s^{-1}$. The UF process feed was an OOWW pre-treated (PR-OOWW) following the protocol presented in other studies [13]. The raw OOWW was collected during the production of olive oil in October 2019 in the Valencian Community (Spain). It was taken at the outlet of the vertical centrifuge after the olive oil washing in the two-phase continuous centrifugation process. The characterization of the PR-OOWW and UF permeate is shown in Table 1.

Table 1: Characterization of samples from pre-treatment stages

	PR-OOWW*	UF Permeate
pH	5.14 ± 0.01	5.19 ± 0.02
Conductivity ($mS \cdot cm^{-1}$)	4.54 ± 0.03	5.35 ± 0.01
Turbidity (NTU[a])	22.80 ± 0.57	0.04 ± 0.00
Suspended solids ($mg \cdot L^{-1}$)	1400 ± 11.02	0.12 ± 0.00
COD[b] ($mg \cdot O_2 \cdot L^{-1}$)	42950 ± 198.12	14580 ± 12.37
TPhC[c] ($mgTyeq \cdot L^{-1}$)	1101.16 ± 16.12	954.78 ± 12.70
SUG[d] ($mg \cdot GluL^{-1}$)	4484 ± 57.37	3730 ± 325.10

[a] NTU: Nephelometric Turbidity Units; [b] COD: chemical oxygen demand; [c] TPhC: Total phenolic compounds; [d] SUG: sugars *PR-OOWW: pre-treated olive oil washing wastewater (OOWW)

Table 2: Specifications of the nanofiltration membranes used

	NF90	NF245	NF270	DM900[#]
Supplier	Dow Filmtech	DuPont	Dow Filmtech	Evonik
Material	TFC[a]PA[b]	TFC[a]PP[c]	TFC[a]PA[b]	ISA[d] Modified PI[e]
Contact angle	53.0[1] - 66.45[2]	11.0[3]	25.4[4]	69.7[5]
MWCO (Da)	90 – 180	300	150 - 340	900[f]
Pore size (nm)	0.38[5] – 0.46[1]	-	0.44[6]	-
Zeta potential at neutral pH (mV)	-17.5[6]	-	-21.6[6]	-
T max (°C)	40	50	45	50

P max (bar)	41	54.8	41	20
pH range	2 - 11	3 - 10	3 - 10	0 - 7
Permeability* ($L \cdot h^{-1} \cdot m^{-2} \cdot bar^{-1}$)	3.80	4.87	12.45	6.32

[#]DM900: DuraMem900; [a]TFC: thin film composite; [b]PA: Polyamide; [c]PP: Polypropylene; [d]ISA: integrally skinned asymmetric; [e]PI: polyimide; [f]Molecular weight cut-off of styrene oligomers dissolved in acetone; * Water, at 25 °C, experimentally determined in this work. [1]: [30]; [2]: [31]; [3] [32] [4][33]; [5]:[34]; [6][35]

Once the necessary volume of UF permeate was reached, it was fed to the NF process, which was carried out in a laboratory-scale plant. This plant operated in full recycling mode and was equipped with a feed tank of 40L and a plunger pump. The membrane module was designed by the research institute ISIRYM [36]. This module allows the use of one flat sheet membrane with an active area of 0.0072 m^2. Four different membranes were tested under different CFV (0.5-1.5 $m \cdot s^{-1}$) and TMP (5 - 15 bar). The specifications of the membranes are presented in table 2.

Every 30 minutes 50 mL of permeate sample was collected for further analysis. The experiments were performed at a constant temperature of 21 ± 1°C, controlled by an electrical resistance and a cooling coil. The performance of the membranes was evaluated by calculating the rejection of the chemical oxygen demand (COD), total phenolic compounds (TPhC) and sugars (SUG), under the following equation (Eq. 2)

$$\%R_J = \left(1 - \frac{C_{pj}}{C_{fj}}\right) \cdot 100 \qquad \text{(Eq.2)}$$

Where *Rj* corresponds to the apparent rejection of the different parameters *j* (COD, TPhC or SUG) expressed in %; *Cpj* and *Cfj* are the concentration of parameter *j* in the permeate stream and in the feed solution, respectively.

2.1.2 Samples analysis

All the samples were characterized for the same parameters. Electrical conductivity was determined by means of a digital calibrated conductivity meter (EC-Meter GLP 31+) and pH by using a pH-meter (GLP 21+), both from Crison (Barcelona, Spain). For turbidity, a D-112 turbidimeter (DINKO, Barcelona, Spain) was used following the UNE-EN ISO 7027 standard method. COD was measured with Merck kits (Darmstadt, Germany) in a range of 500-10.000 $mg \cdot L^{-1}$ and the measurement of suspended solids was performed following the UNE 77034 standard method from APHA [37]. Total phenolic compounds concentration was determined by means of the Folin-Ciocalteau method [38] with tyrosol (VWR Chemicals, USA) as standard. Sugar concentration was determined by the Anthrone colorimetric method [39], whit glucose (Panreac, Barcelona, Spain) as standard.

2.1.3 Cleaning protocol

The membranes were cleaned after each test to remove fouling. Firstly, tap water was flushed through the system for 5 minutes. The cleaning procedure consisted of four successive steps, only performing the steps needed to recover the initial permeability of the membrane by at least 95%. The duration of each step was 30 minutes. The protocol steps were the following: C1: pure water at 25°C, C2: pure water at 35°C, C3: 1%v/v Ultrasil solution at 25°C and C4: 1%v/v Ultrasil solution at 35°C. The last two solutions for the chemical cleaning were prepared with P3 Ultrasil 115 (Ecolab, Barcelona, Spain).

2.2 Analysis with 2D fluorescence spectroscopy and FTIR

The diagram plotted in figure 1 shows the methodology followed for the analysis of the effect of fouling and cleaning of the membrane surface with 2D fluorescence spectroscopy and FTIR. Each stage is explained separately below.

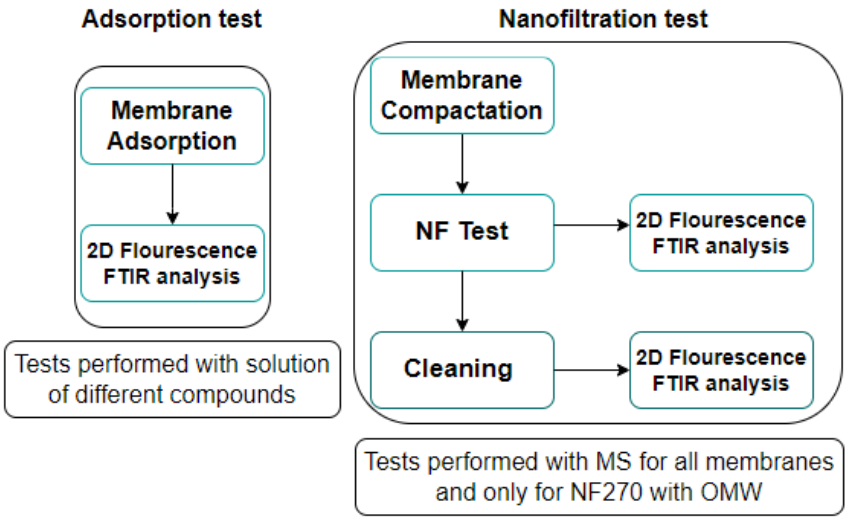

Fig. 1. Methodology to evaluate the effect fouling and cleaning of the membranes with 2D fluorescence spectroscopy and FTIR. NF: nanofiltration; MS: model solution; OMW: olive mill wastewater

2.2.1 Adsorption tests

First, adsorption tests were performed with all the membranes. The four membranes were evaluated in the same way under the following protocol: a piece of membrane (3x3 cm) was immersed in different solutions for 24 hours to further analyse the surface of the membranes by 2D fluorescence and FTIR spectroscopy, in order to find out whether some compounds were adsorbed by the membrane. The compounds (supplier by BioNova Científica (Spain) and PanReac Applichem (Spain)) selected for the adsorption tests were based on the composition of the real OOWW used [40]. One compound of each family (chemical class) was selected: citric acid (CI) corresponding to organic acids, caffeic acid (CA) corresponding to phenolic acids,

hydroxytyrosol (HT) representing simple phenols, luteolin (LUT) to flavonoids and a mixture of glucose, fructose and sucrose to sugars (SUG). It is important to emphasize that the adsorption assay did not consider the actual concentrations of each compound present in the OOWW, but the aim was to use the same concentration for each compound. With the exception of sugars, the concentration of each compound in distilled water solutions was 20 ppm (conductivity <70 μS/cm). The sugar solution had a concentration of 30 ppm, with 10 ppm of each compound. As a control, it was decided to leave a piece of membrane in distilled water. On the other hand, other pieces of membrane were also immersed in a solution with the chemical reagent used in chemical cleaning (P3 Ultrasil 115, 1% v/v). This followed the same adsorption protocol as the membrane pieces in the different solutions. This is done to analyze if there were changes in the membrane surface after cleaning (also acts as a control).

2.2.2 Nanofiltration tests for membrane fouling analysis

For these NF tests, a model solution (Table 3) made with the same reagents used for adsorption analysis was used as feed stream. In this case, the concentration of each compound was consistent with the concentration obtained from the liquid chromatography–mass spectrometry characterization of the real OOWW, which can be found elsewhere [40]. A new model solution was used for each test. The tests were carried out under the best operating conditions ($1 m \cdot s^{-1}$ of CFV and 10 bar of TMP) that were selected after a previous study with OOWW (section 2.1). These tests were carried out in another nanofiltration plant. In this case, the plant was assembled with a GE-Sepa CF module (GE OSmonic, Minnetonka, USA) and a Hydra-cell G13 model pressure pump (Wanner Engineering Inc., Minneapolis, USA). The NF active membrane area was 0.014 m^2. Permeate and concentrate samples were collected after half an hour and at the end of the test and stored for future analysis.

Table 3. Characterization of model solution used as feed in the nanofiltration tests

Compound	Family (Chemical class)	Concentration (ppm)
Citric acid	Organic acids	207.10 ± 1.06
Caffeic acid	Phenolic acids	4.22 ± 0.05
Hydroxytyrosol	Simple phenols	3.43 ± 0.16
Luteolin	Flavonoids	3.33 ± 0.02
Glucose	Sugars	700.02 ± 0.02
Fructose	Sugars	100.35 ± 0.01
Sucrose	Sugars	100.67 ± 0.02

Upon completion of the assay, the membrane was removed from the module and 2D fluorescence was measured immediately to avoid drying out of the membrane. The FTIR spectra of the

membrane was also determined after the test. The membranes were stored in a refrigerator (5°C) to avoid their degradation.

To analyse the effectiveness of the cleaning protocol, the test explained above was repeated, but, this time, followed by a chemical cleaning. For this, the cleaning protocol that presented the best results at the time of recovering the initial permeate flux in the OOWW test was used (C4: 1%v/v Ultrasil solution at 35°C). First, the membrane was rinsed with tap water for 5 minutes, before circulating the cleaning solution for 30 minutes under a TMP of 1 bar at 35°C (same protocol presented in 2.1.3.). The membrane was then rinsed with distilled water to remove all chemical residues and afterwards the 2D fluorescence of the membrane surface was immediately measured. As mentioned above, the membrane was later analysed with FTIR spectroscopy, keeping it refrigerated to avoid degradation.

Finally, a NF test was performed with OMW using only the membrane that showed the best results in the study with OOWW. The OMW sample was provided by Zeyton Nutraceuticals, Portugal from a three-phase continuous centrifugation process. The sample was treated following the same protocol as that applied for the OOWW. Then, it was diluted to obtain a composition similar to that presented by OOWW. The operating conditions for both the NF test and the cleaning protocol were the same ones describe above. The membrane was also evaluated under 2D fluorescence and FTIR spectroscopy after the NF test. Finally, a chemical cleaning was performed.

2.2.3 2D fluorescence and FTIR spectroscopy

The fluorescence spectra of the membranes and samples were acquired with a Varian Cary Eclipse fluorescence spectrophotometer equipped with excitation and emission monochromators and coupled to an optical fibre bundle probe. The excitation-emission fluorescence spectroscopy measurements (EEMs) were obtained at a scan speed of 12000 $nm \cdot min^{-1}$, and excitation and emission slits of 5 and 10 nm, respectively. Fluorescence spectra were determined in a wavelength range of 245 and 745 nm of excitation and an emission wavelength range between 250 and 750 nm with an incrementing step of 5 nm. FTIR spectra of the membranes were obtained utilizing Shimadzu IRAffinity-1S in absorption mode from 400 to 4000 cm^{-1} with 4 accumulations scans and a resolution of 10 cm^{-1}. Furthermore, the data obtained by these techniques was deconvoluted and compressed into some major PCA components (Supplementary material, section 1) for better analysis.

3. Results

3.1 Membrane characterization and permeate fluxes in nanofiltration tests for process optimization

The measured hydraulic permeability values agree with the data obtained by other authors [28,41,42], with the NF270 membrane exhibiting the highest permeability (12.45 $L \cdot h^{-1} \cdot m^{-2} \cdot bar^{-1}$) and the NF90 membrane the lowest one (3.80 $L \cdot h^{-1} \cdot m^{-2} \cdot bar^{-1}$). No record of the water permeability

of the DuraMem900 (DM900) membrane was found in the literature. The hydraulic permeability for the other membranes were 6.32 $L \cdot h^{-1} \cdot m^{-2} \cdot bar^{-1}$ and 4.87 $L \cdot h^{-1} \cdot m^{-2} \cdot bar^{-1}$ for DM900 and NF245, respectively.

Fig. 2 shows the mean permeate flux values for the different operating conditions tested in the NF experiments with OOWW. The error is not presented, but in all cases it was less than 9%. In general, it is observed that permeate flux was more affected by TMP, showing a linear increase with TMP for all the CFVs tested. However, this behaviour was not observed in all tests. For the NF90 and DM900 membranes, the permeate flux presented a deviation from linearity at high TMPs (above 10 bar). This may be explained because the critical flux is being reached, which is evidence of membrane fouling [43]. In the case of the DM900 membrane, similar flux values were obtained at 10 and 15 bar, which was more noticeable at low CFV. This may be due to the fact that high TMP values could contribute to concentration polarization [44], which would result in a greater flux decrease (in this case from 10 bar). Higher flux values were obtained at higher CFV conditions. The decrease in flux is mainly due to the formation of a gel layer or cake. Thus, increasing CFV allows improving the transfer of solids present on the membrane surface back into the bulk stream [45]. Therefore, a reduction in the thickness of the fouling layer occurs, with the subsequent increase of the permeate flux. It also allows working at higher TMP values. On the other hand, in nanofiltration, especially at high TMP, the effect of the osmotic pressure gradient may be relevant. The accumulation of inorganic or organic solutes generates an increase in the osmotic pressure difference between the two sides of the membrane and will lead to the reduction of the effective TMP and the permeate flux [12,46]. Mohammad et al. [46] pointed out that while studies of fouling mechanisms have been conducted, it remains difficult so far to predict which mechanism is involved.

The lower hydraulic resistance to water transport exhibited by the NF270 membrane due to its relatively loose semi-aromatic skin rejection layer may explain the high permeate fluxes [47]. The DM900 was the membrane that presented the greatest hydraulic resistance, due to the more hydrophobic properties of the modified polyimide [34] in comparison to the other membranes materials. Also, when comparing the hydraulic permeability and the permeate flux with the OOWW, this membrane (DM900) was the one that presented the greatest difference, showing a flux decrease between 56-65% (depending on the TMP), which could infer that this membrane was the most affected by fouling. Similar results were observed by Böcking [48] when using a membrane of the same material (DuraMem500). They observed that the addition of PEG as a solute generated a significant decrease in permeate flux (close to 45%). They attributed it primarily to concentration polarization effects.

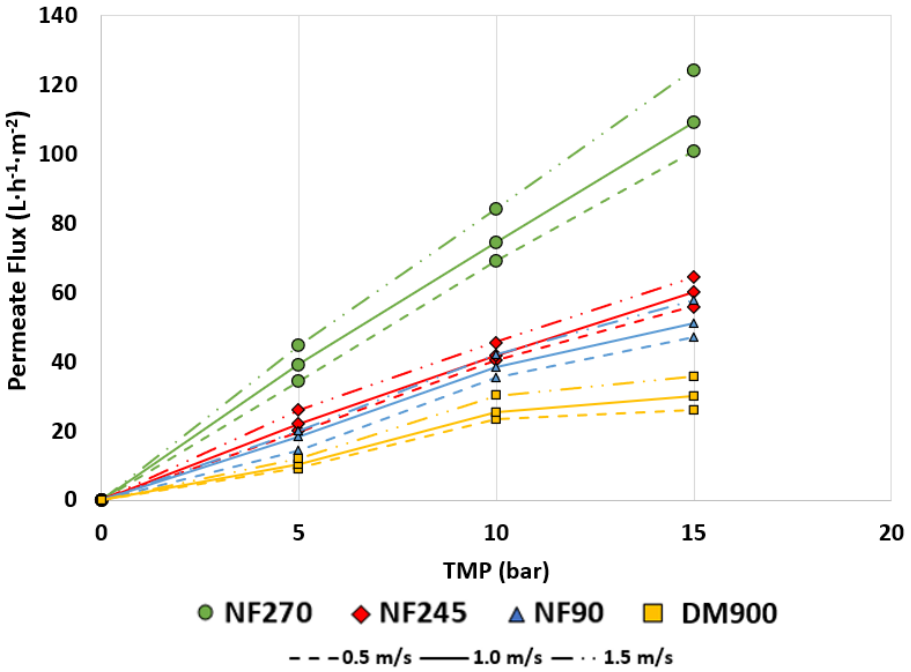

Fig. 2 Stationary permeate flux obtained at the different TMP and CFV during the nanofiltration of olive oil washing wastewater

[colour figure]

It has been usually reported that permeate flux affects permeability reduction because the higher the flux, the faster the accumulation of solutes on the membrane surface [49,50]. However, a linear relationship between higher permeate flux values and higher fouling was not observed (Fig. 3). The membrane with the highest permeate flux (NF270) was found to exhibit relatively similar fouling to those of the NF245 and DM900 membranes in terms of permeate flux decline over time. This could indicate a non-severe fouling in the NF270 membrane. Once again, it can be seen how the DM900 membrane was the most affected by fouling, due to its constant flux decrease, being the last to reach a steady state. On the other hand, the membrane with the lowest MWCO reached faster the stationary permeate flux, which could be due to rapid fouling. Nunes et al. [47], in their study on the extraction and concentration of bioactive compounds from olive pomace using membranes, observed a similar performance of the NF90 membrane, attributing it to the polymeric structure of the membrane. This membrane is open enough to let the foulants penetrate through the membrane, but, at the same time, it is closed enough to generate a close/block in one step, generating a rapid decrease in flux prior to a flux stabilization. Similarly, as in this study, these authors observed an opposite behaviour with the NF270 membrane, which suffered from progressive fouling. As the intra-polymeric voids in its active layer are too large to block them all at once, flux decay is not so abrupt as in the case of NF90 membrane.

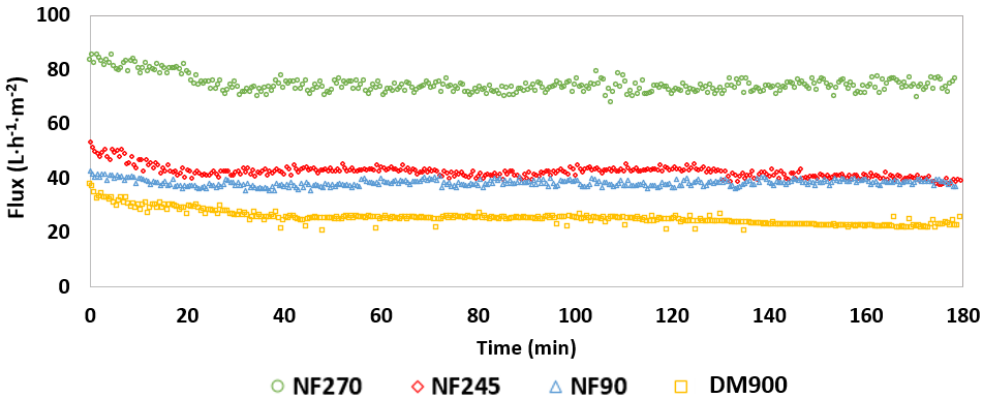

Fig. 3 Variation of permeate flux over time in OOWW nanofiltration at a TMP of 10 bar and CFV of 1 $m \cdot s^{-1}$

[colour figure]

3.2 Membrane rejections

Fig. 4 shows the percentages of rejection obtained in the NF tests performed. In all tests, an increase in rejection percentages can be seen with increasing TMP as expected. Regarding the CFV, rejection seemed to increase at increased CFV values. However, this behaviour did not repeat for all the membranes. At a fixed TMP of 10 bar, the NF245 membrane had the highest rejections for all the compounds at 1 $m \cdot s^{-1}$. Therefore, the increase in CFV generated a decrease in the rejection efficiency for this membrane. This could be due to the aforementioned effect of fouling layer diminution by increasing CFV, and better external mass transfer conditions (lower concentration polarization). This fouling layer could act as an additional layer, generating additional resistance to the pass of the solute through the membrane [51].

The NF90 membrane was the one that presented the highest COD retention percentages, while the DM900 had the lowest. This agrees with the retentive properties of these membranes, with the NF90 being the one with the lowest MWCO. On the other hand, although according to the manufacturer, both NF245 and NF270 membranes exhibit similar MWCO, the higher retention exhibited by the NF270 suggested a tighter top layer structure than that of the NF245.

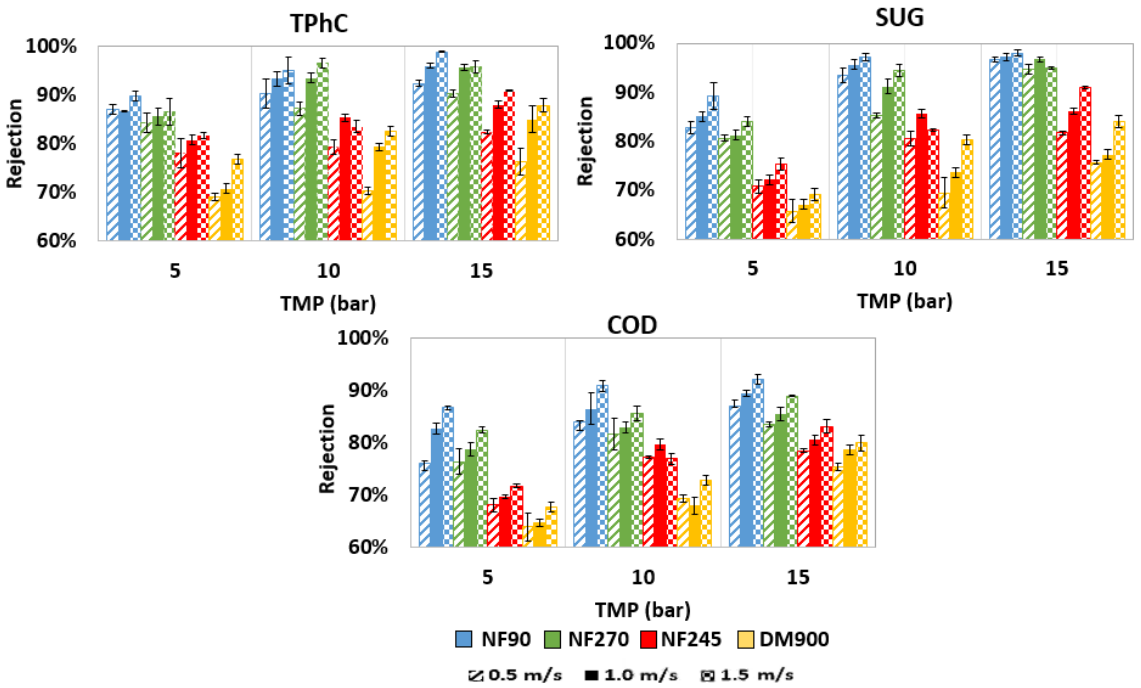

Fig. 4 Steady state rejection of TPhC (total phenolic compounds), SUG (sugars) and COD in the nanofiltration of olive oil washing wastewater

[colour figure]

Interesting results were obtained with the DM900 membrane. Although low permeate fluxes were obtained, the percentages of phenolic compounds rejection are within the range of the other membranes. Although this membrane was manufactured for use with organic solvents, the cross-linking reaction that occurs in its manufacture generates an increase in hydrophilicity, with a contact angle indicating a polar active layer [48], therefore it is suitable for use in aqueous solutions. Other studies have shown great rejection of total phenolic compounds in organic solvent solutions (near 80%) using this membrane [34]. In this case, the rejections were similar and in some cases higher; this may be due to the fact that for hydrophilic membranes the rejections in water will be higher than in organic solvents [52]. Although, the NF90, NF245 and NF270 membranes presented similar rejection ranges for phenolic compounds, the NF270 was by far the one that presented the highest permeate flux in all tests carried out. Thus, this membrane was found to be the most appropriate for the concentration of phenolic compounds from OOWW. Similar results were observed by López-Borrell et al. [53] in the recovery of phenolic compounds from wine lees. Although the rejection of the phenolic compounds that presented the NF90 and NF245 membranes was high, they showed very low permeate flux values. Also, the zeta potential (table 2), can be related with the higher rejections presented by NF90 and NF270 membrane. It can be due to higher cross-linking of the aromatic polyamide (as deduced from zeta potential measurements), which corresponds to higher polymer density and hindered diffusion of the solute

[54]. Therefore, the NF270 membrane was selected as the optimal one because it presented the highest values of permeate flux with a rejection of phenolic compounds above 93%. It is important to highlight that no interactions between the membranes and the phenolic compounds are expected. Due to the pH of the OMW, the membranes are negatively charged (isoelectric point, 4.0 - 5.0 [28,55–57]), and the phenolic compounds are found in their deprotonated form at basic pHs, which is not the case.

The rejection of sugars showed a similar trend to the rejection of phenolic compounds, with all membranes presenting high percentages of sugar rejection. The increase of TMP from 5 to 10 led to a significant increase in rejection. This was also observed by Nguyen et al. [58], who studied the use of NF and RO for the detoxification of lignocellulosic hydrolysates. They observed that when TMP was raised at values higher than 10 bar glucose rejection increased (>94%), regardless of the membrane analysed. Although only glucose was considered, about 60% of the sugars present in OOWW correspond to glucose, so the trend can be extrapolated to the sugars analysed in this study. On the other hand, the permeate obtained by all membranes was adequate to be reincorporated into the process as machinery cleaning water, with low COD and TPhC. Ochando-Pulido et al. [59] also obtained high COD rejection (86.76%) with the 300Da DK membrane (GE Water & Process Tech) when working with OOWW. These authors used the permeate (practically without phenolic compounds) for irrigation.

3.3 Membrane cleaning

The recovery of the hydraulic permeability of the membranes after each test and the cleaning protocols performed are shown in Fig. 5 (A and B). It can be seen that from the 4th use of the membranes there was a decrease in the permeability recovery percentage for most of them (Fig. 5A). This was more significant for the NF90 and DM900 membranes. This could be explained because these tests were performed above sustainable flux conditions, as they were performed at high values of TMP. This term is related to the permeate flux value that corresponds to non-severe fouling an to a profitable balance between investment and operating costs [60–62]. Therefore, the operating conditions generated high fouling, which made cleaning difficult, hindering the recovery of the hydraulic permeability. In this case, working with the NF90 and DM900 membranes under the conditions of tests 4-9 would imply the need for a more aggressive cleaning, as high TMP and low CFV values were considered for these tests, thus increasing membrane fouling. This could result in higher spending of chemical reagents for cleaning or more energy to raise the temperature. On the other hand, the NF245 and NF270 membranes were the only ones capable of recovering permeability in all tests by at least 95%. It is important to note that these two membranes mostly present reversible fouling, managing to recover an average of 86.7 ± 3.8% and 82.3 ± 4.1% after C1, which was performed with water at room temperature. Membrane materials and feed solution also play an important role in the reversibility/irreversibility of the

fouling process. In this case, the interaction between the membrane material and foulants was higher for the NF90 and DM900 membranes than for the others, making fouling removal more difficult. Although the NF270 and NF90 membranes are made of the same material, the NF90 exhibited high fouling. Similar results were obtained by Arboleda Mejia et al. [42], who only recovered 60% of the initial water permeability of this membrane when it was used to recover phenolic compounds from red grape pomace. They attributed it to the possible adsorption of phenolic compounds, which tends to irreversible. This will be discussed in the next section, where the results of the adsorption tests will be commented.

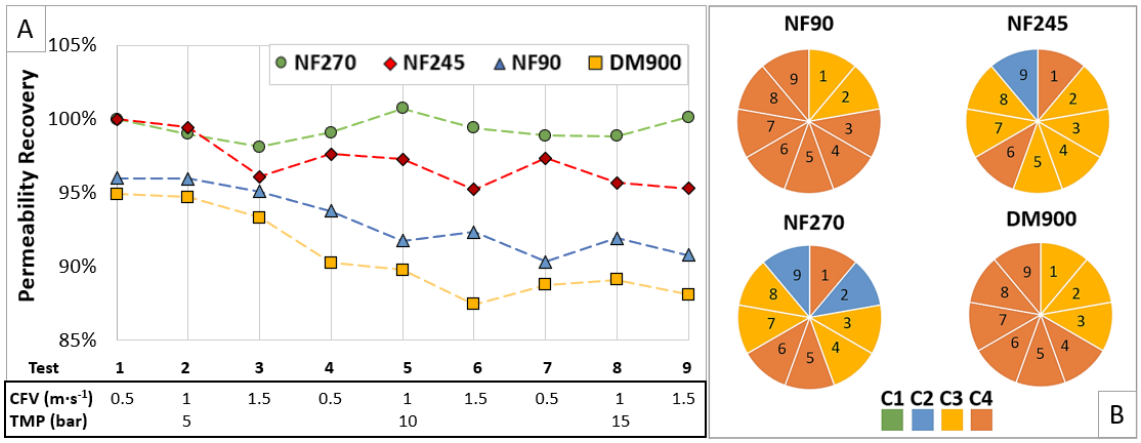

Fig 5. A: recovery of the initial hydraulic permeability after cleaning. B: cleaning protocol necessary to achieve the hydraulic permeability recovery in each test (1-9) indicated in figure A; C1: water at 25°C, C2: water at 35°C, C3: chemical cleaning with P3 Ultrasil 115 (1% v/v) at 25°C and C4: P3 Ultrasil 115 (1% v/v) at 35°C.

[colour figure]

In fig.5B, it can be seen that almost all the tests required chemical cleaning (protocol C3 and C4) to recover the initial hydraulic permeability, which means that fouling was mainly irreversible. For the NF245 and NF270 membranes, the cleaning protocol proposed was successful. However, the NF90 and DM900 membranes would require a more exhaustive cleaning for a higher permeability recovery.

As a general conclusion for sections 3.1, 3.2 and 3.3, it can be stated that the NF270 membrane showed the best performance for the studied application. Under the operating conditions of 1m·s^{-1} of CFV and 10 bar of TMP, it yielded a stable permeate flux of 74.4 L·h^{-1}·m^{-2}, a rejection of total phenolic compounds of 94% and a COD rejection of 83%.

3.4 Adsorption tests

Figures 6-9 present the contour spectra obtained with 2D fluorescence spectroscopy for the adsorption experiments. In all the figures, the emission (Em) wavelength (in nm) is plotted on the "x" axis and the excitation (Ex) wavelength (in nm) on the "y" axis. The fluorescence intensity is also shown through colours, with the yellow colour representing the highest intensity.

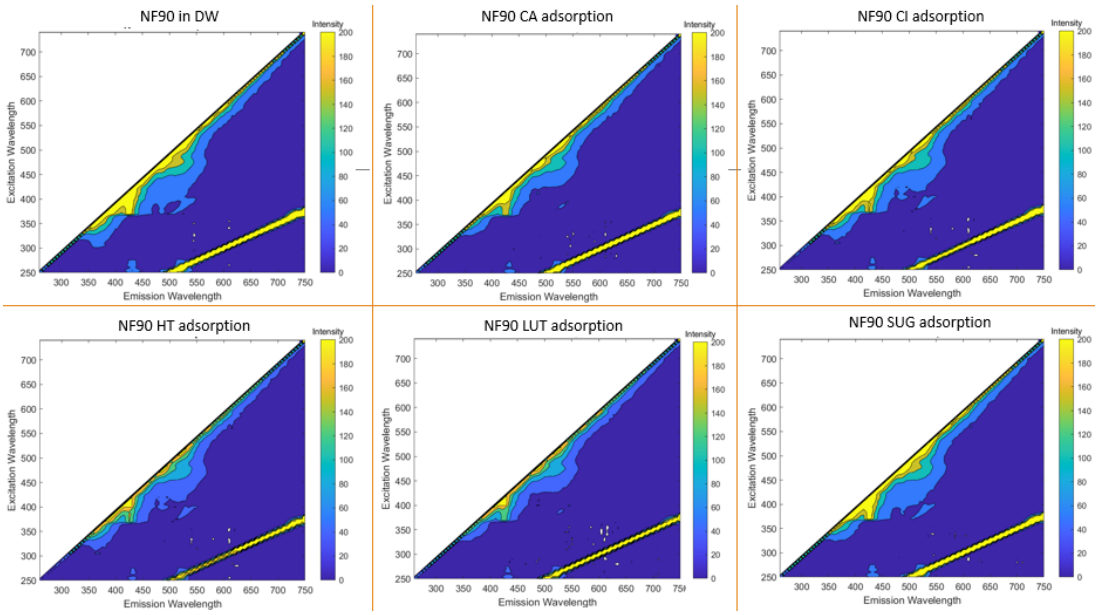

Fig.6 2D fluorescence spectra for the adsorption test performed with the NF90 membrane. DW: deionized water; CA: caffeic acid; CI: citric acid; HT: hydroxytyrosol; LUT: luteolin; SUG: sugars

[colour figure]

Fig. 6 shows the spectra obtained for the NF90 membrane. The membrane Ex/Em characteristic region (NF90 in deionized water (DW)) was between 325-525/350-575 nm. With the exception of SUG, the contact with the different compounds during adsorption studies slightly affect the characteristic signal of the membrane between the Ex/Em lengths of 400/450 nm. However, due to the low fluorescence signal of the membrane it is difficult to see differences between the compounds tested. The DM900 membrane (Fig. 7) showed similar results as the NF90 membrane. A fluorescence signal characteristic of the membrane was observed in all DM900 adsorption experiments. The low intensity of the signals may be due to the nature of the membrane, specifically the material from which it is made. In this particular case, the DM900 membrane has an intense brown colour, indicating light absorption, contributing to the low signal intensity. Nevertheless, CA clearly affected the signal of the membrane, followed by LUT.

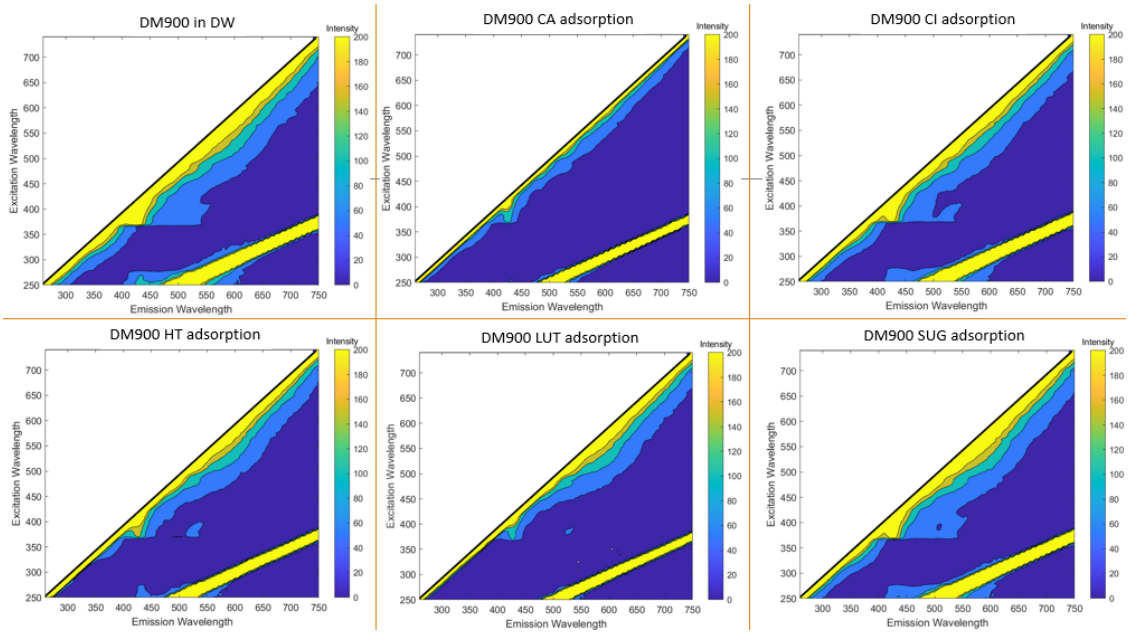

Fig. 7 2D fluorescence spectra for the adsorption test performed with the DuraMem900 (DM900) membrane. DW: deionized water; CA: caffeic acid; CI: citric acid; HT: hydroxytyrosol; LUT: luteolin; SUG: sugars

[colour figure]

A very different result was obtained with the NF245 and NF270 membranes (Fig. 8 and 9, respectively). A strong characteristic Ex/Em signal between 300-450/325-475 nm was observed for both membranes. Clearly, a great influence of LUT and CA was observed on the signal, completely overshadowing the NF245 membrane signal. This means that these compounds have being adsorbed by the surface of the membrane, hiding the characteristic signal of the membrane. Although CI did not completely eliminate the signal of the NF245 membrane, it did affect it, reducing its intensity. For the NF270 membrane no changes in the signal were observed with CI. Moreover, HT and SUG did not cause clear changes in the characteristic signal of both membranes. These results show that either these compounds are little or no adsorbed by the membrane surface or that they do not induce visible changes in the fluorescence spectra. In fact, besides the natural fluorescence ability, the natural colour of some compounds can affect the signals emitted by the membrane surface and may alter the membrane surface colour [21]. Therefore, the coloured compounds can be easily detected, more than the non-coloured compounds (HT - CI - SUG). Nevertheless, the effect of CI on the NF245 membrane signal points out a higher impact of CI on this membrane than on the other 3 membranes tested.

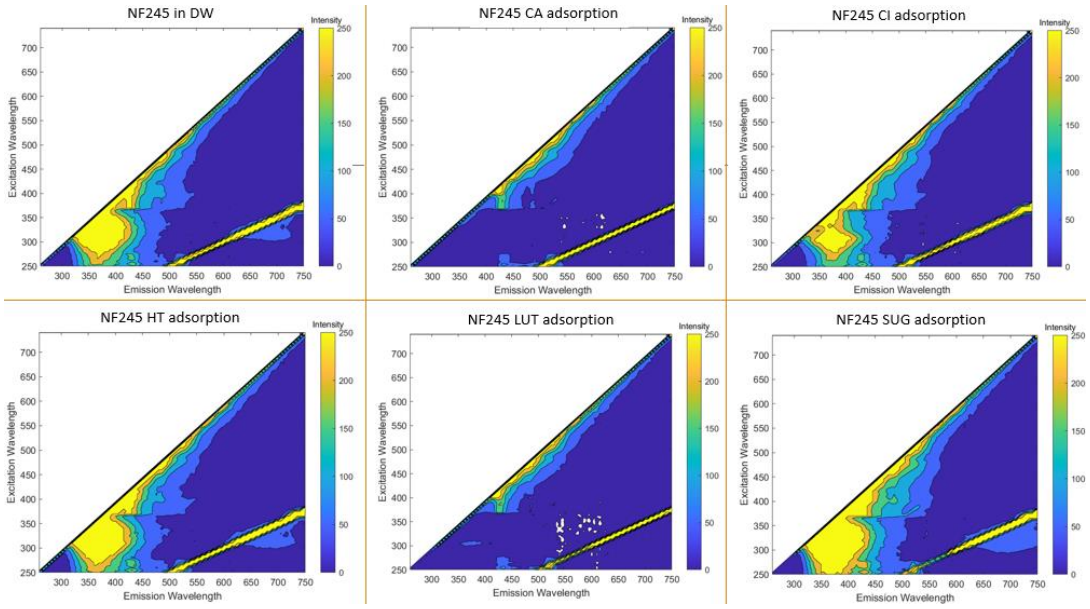

Fig. 8 2D fluorescence spectra for the adsorption test performed with the NF245 membrane. DW: deionized water; CA: caffeic acid; CI: citric acid; HT: hydroxytyrosol; LUT: luteolin; SUG: sugars

[colour figure]

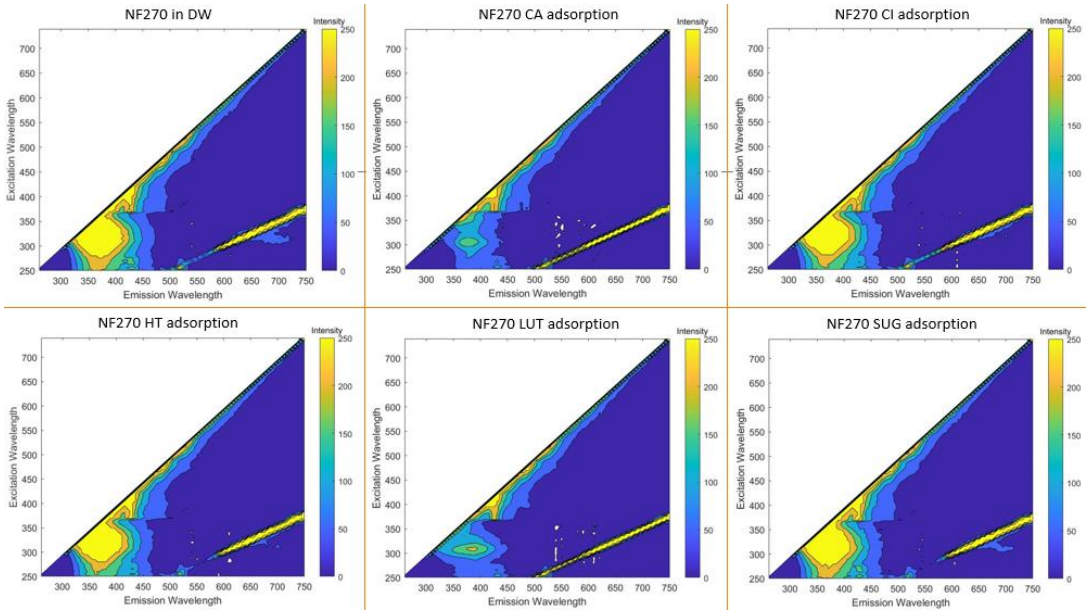

Fig. 9 2D fluorescence spectra for the adsorption test performed with the NF270 membrane. DW: deionized water; CA: caffeic acid; CI: citric acid; HT: hydroxytyrosol; LUT: luteolin; SUG: sugars

[colour figure]

To better understand the effect of the compounds tested on the membrane surface, the results will be analysed together with the FTIR spectra.

The FTIR spectra acquired for the membrane surfaces exposed to the different compounds can be compared with the spectra of the original membrane (only exposed to deionized water). The impact of each compound is reflected not only by changes on the spectrum profile (different peaks), but also through the effect on the characteristic peaks from the original membrane. In all graphs, the "x" axis represents the intensity of the infrared spectra (cm^{-1}); and the "y" axis represents the amount of infrared light transmitted by the material being analysed (% Transmittance (T)), which is inversely related to absorbance.

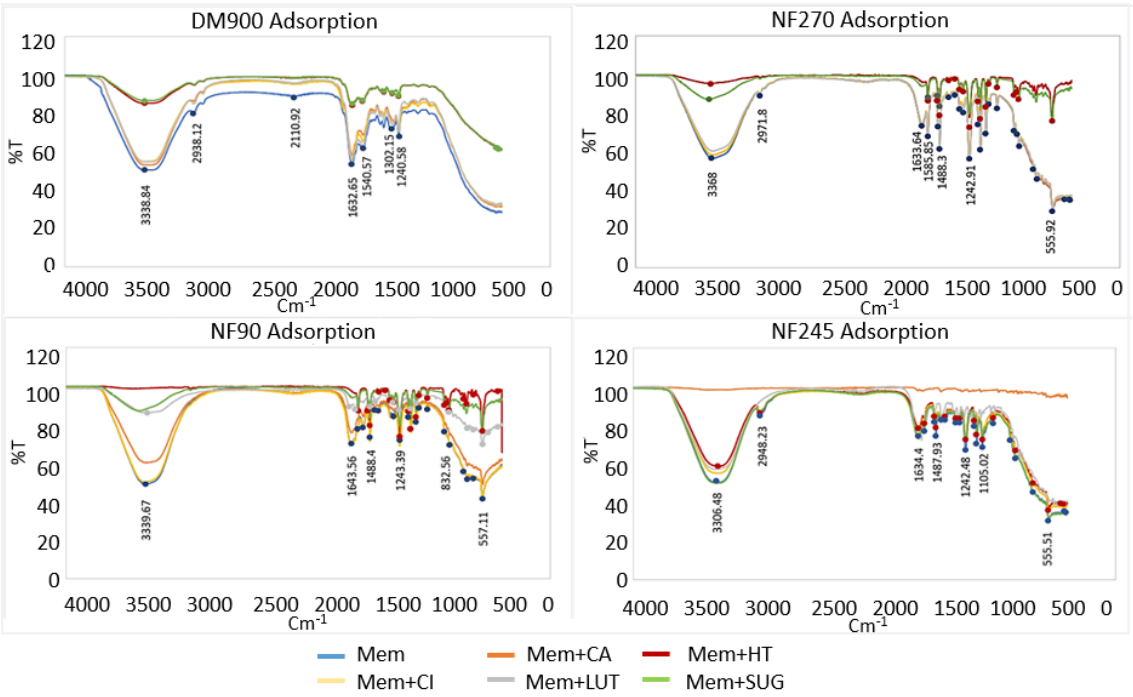

Fig. 10 FTIR spectra for all the membrane tested. Mem: Pristine membrane; CA: caffeic acid; CI: citric acid; HT: hydroxytyrosol; LUT: luteolin; SUG: sugars

[colour figure]

It can be seen in Fig. 10 that the NF90 and NF270 membranes have similar specific peaks due to the material, three of them being the most characteristic, around 555-557 cm^{-1}, 1643-1633 cm^{-1} and 3368-3339 cm^{-1}, respectively. The range between 500 and 900 cm^{-1} is attributed to aromatic rings, the peak around 1600 cm^{-1} can be due to aromatic C=C stretching, while the peaks around 3300-3400 cm^{-1} can be attributed, besides the -COH group, to stretching vibration between the carboxyl group (-COOH) of polyamide (PA) layer and N-H [63]. The N270 membrane presents also a characteristic peak at 2971.8 cm^{-1}, that can be due to CH_2 asymmetric stretching [33]. Both membranes present a complete elimination of the signal in the presence of HT, followed by SUG, indicating that both compounds have been adsorbed. This could be explained by the membrane material, as both membranes are made of polyamide, being more susceptible to the adsorption of

these compounds. Cassano et al. [64,65], when artichoke brine was nanofiltered with a PA membrane (Desal DK, from GE Osmonics), observed that when the volume reduction factor (VRF) increased the concentration of chlorogenic acid and caffeoylquinic acid derivatives did not proportionally augmented. They pointed out that it was due to different factors, one of which was the adhesion of these compounds to the membrane. Our observation could be explained taking into account that HT is more hydrophobic than another non-adsorbed compound such as citric acid (octanol-water partition coefficient (Log P) of 0.96 [66] and −1.99 [67] for HT and citric acid, respectively). Lopez-Muñoz, et al. [35] reported that this is the main parameter to describe the adsorption of phenolic compounds on nanofiltration membranes. When analysing the NF90 membrane, they observed that the hydrophobicity (log P) of the phenolic compounds was directly related to the adsorption of the solute on the membrane surface.

The NF90 membrane also showed an adsorption of LUT similar to that of SUG and a slight CA adsorption. This could also be explained trough the hydrophobicity character, since LUT and CA present a Log P similar to HT (0.7 [68] and 1.3 ± 0.240 [69] for LUT and CA, respectively). However, this was not observed for the NF270 membrane. Although both are made of polyamide, it has been reported that the NF90 membrane material is an aromatic polyamide, while the NF270 is a mixed aliphatic-aromatic polyamide membrane. This indicates that the NF90 membrane surface is rough, while the NF270 membrane shows a smooth surface [70]. The "peak-valley" morphology at the surface of the roughened membranes results in a higher specific surface area. Thus, the adsorption capacity would be larger for membranes with rougher surfaces [50]. This could also explain the difficulties encountered when cleaning this membrane (section 3.3). Corbatón-Báguena et al. [71] also reported in their study of saline solutions for cleaning ultrafiltration membranes fouled with BSA, that the greater the roughness, the greater the difficulty in cleaning the membranes. On the other hand, the NF245 membrane shows the characteristic signals of the material (PP). Vibrations of the –CH, $–CH_2$ and $–CH_3$ groups were observed, such as the methyl absorption band between 1242 and 1487 cm^{-1}. C-H bonds were detected at around 2948 cm^{-1} and the characteristic peak of hydroxyl groups at around 3000 – 3600 cm^{-1} [72]. The FTIR spectrum of the NF245 membrane submerged in CA showed a transmittance higher than 95%T for all the wavelengths, being the only compound that caused changes in the characteristic signal of the membrane. Except for the SUG, the other compounds show a slightly increase in %T. LUT, on the other hand, overshadows the characteristic signal of C-H at 2948 cm^{-1}.

The most characteristic peaks of the DM900 membrane corresponded to the imide (1720 and 1237 cm^{-1}) and also amide group (1632 and 1530 cm^{-1}) due to crosslinking [73]. As in the case of the NF90 membrane, by means of FTIR, it was possible to corroborate that there is adsorption of some compounds on this membrane, being the SUG and the HT the ones that presented the highest

impact. On the other hand, the other compounds, although they had less impact on the membrane surface, all of them caused a slight increase in transmittance in the range of 3000 - 1600 cm^{-1}, demonstrating that there was adsorption.

It can be concluded that the fluorescence spectra acquired on NF90 and DM900 membrane surfaces had low signal intensity and changes caused by possible adsorption of foulants were not clearly visible by direct visual inspection. The PCA of the obtained fluorescence response (supplementary material, Fig. S1) showed that the DM900 membrane was affected by both CA and LUT. This is because the presence of such compounds can be detected not only due to a shadow effect (possible quenching effects), but also by spectral changes due to their natural fluorescence (even if these differences are not clearly seen on the spectra) [74]. Regarding NF90, it presented a significant fluorescence difference from the other membranes, and besides, the differences with the membranes exposed to the compounds were not so evident (most probably due to low fluorescence signal captured for this membrane). All measurements clustered differently in the PCA plot, showing clear differences for membrane surfaces exposed to the compounds. NF270 and NF245 surfaces have similar spectra and the effect of the compounds was similar on both, with CA and LUT being the compounds that most affected the membranes. These conclusions were confirmed with PCA analysis.

With FTIR it was possible to observe that the NF90, NF270 and DM900 membranes were the most affected by HT and SUG, while the NF245 membrane was mostly affected by CA. In FTIR PCA analysis (Supplementary material, Fig. S2), the similarity between the composition of all membranes is clear and the differences in the membrane surfaces were not captured (such as the brown colour of DM900). However, the DM900 membrane shows a different behaviour when exposed to the selected compounds, being clearly affected by all the compounds. While fluorescence analysis showed a more pronounced response for CA and LUT, from FTIR it was possible to see more clearly the effect of the other compounds tested. Based on both methods, it can be determined that all the compounds had an effect on the membrane surfaces, meaning that all were adsorbed on the 4 membranes. However, the DM900 membrane was clearly the membrane most affected by all compounds studied.

It was shown that using these techniques it is possible to determine changes on the membrane surface due to fouling caused by adsorption. The 2D fluorescence spectroscopy was useful to determine the adsorption of coloured compounds, while FTIR was able to evaluate the adsorption of colourless compounds and demonstrated that there was adsorption on the NF90 and DM900 membranes. Finally, it can be concluded that both techniques together are a powerful tool when analysing possible changes on membrane surfaces, induced by fouling.

To analyse the membranes with FTIR it is necessary to remove them from the module. However 2D fluorescence spectroscopy is very sensitive and non-invasive, being suitable for in situ

monitoring [75]. 2D fluorescence spectroscopy can be assessed using an optical probe directly from membrane surface using a membrane module with a window. This will be explored in future studies.

3.5 Nanofiltration study: 2D Fluorescence spectroscopy and FTIR

Fig. 11 shows the fluorescence spectra of all membranes after the NF test with MS (fouled membranes with model solution) and after cleaning. As was indicated in section 2.2.2, the operating conditions of all the nanofiltration tests carried out to evaluate the spectroscopic techniques were the same, 3 hours of test at CFV of 1 ms-1 and TMP of 10 bar. Due to fouling, the membranes reduced their fluorescence emission compared to pristine membranes (fluorescence of pristine membranes is shown in section 3.4). This is because the compounds present at the fouling layer can partially absorb the light emitted by the surface of the membrane, attenuating its signal [76]. Regarding the initial spectra of the membranes, the NF245 membrane was the one that presented the highest attenuation. Avram et al. [41] observed in their study on the concentration of polyphenols from blueberry pomace extract using NF245 and NF270 membranes, that the application of mechanical agitation can interrupt the agglomeration or adsorption of polyphenols. When comparing the two membranes, the effect was more pronounced for the NF270 membrane than for the NF245 one. They attributed it to the more compact polymeric structure of the active separation layer of the latter membrane, inducing a larger interaction surface between the polyaromatic membrane moieties and the polyphenols, which could generate a greater adsorption of these compounds.

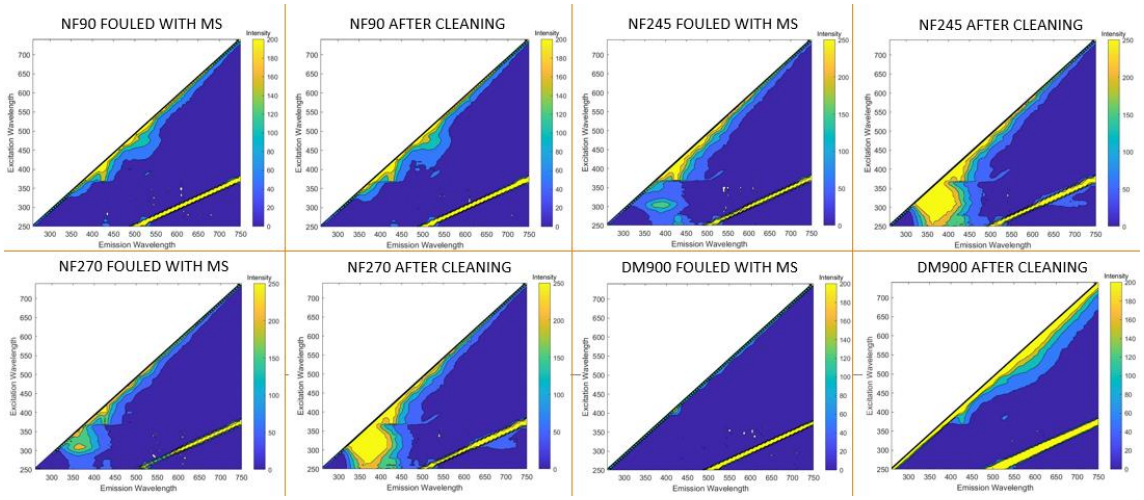

Fig. 11. 2D fluorescence data of the membranes after nanofiltration test with the model solution (MS) and after chemical cleaning. Operating conditions of nanofiltration test, 3 hours at CFV of 1 ms^{-1} and TMP of 10 bar.

[colour figure]

Although at a first glance analysis of the data obtained, all membranes managed to recover their initial fluorescence after applying the cleaning protocol, they did not manage to emit the same signal as the pristine membranes. This can be seen through the analysis of PCA (Fig. 12), where it is also observed that they are more similar to the samples of the new membranes after being subjected to the cleaning protocol. This may be due to the removal of chemicals used to preserve the membranes after the initial membrane cleaning, thus changing the characteristic signal. Simon et al. [77], in a study on the impact of chemical cleanings (acid and basic) on the NF270 membrane surface, presented the hypothesis that cleanings might alter the tightness of the polymeric matrix and even the hydrophilicity of the active layer of the membrane.

These results can be related to those obtained in section 3.3 on membrane cleaning (Fig 5). It can be observed that those membranes that show a greater proximity between the pristine cleaned membrane and the membrane cleaned after the NF test in the PCA, correspond to the membranes with the highest permeability recovery ratio in Fig. 5A, following the order NF270>NF245>NF90>DM900.

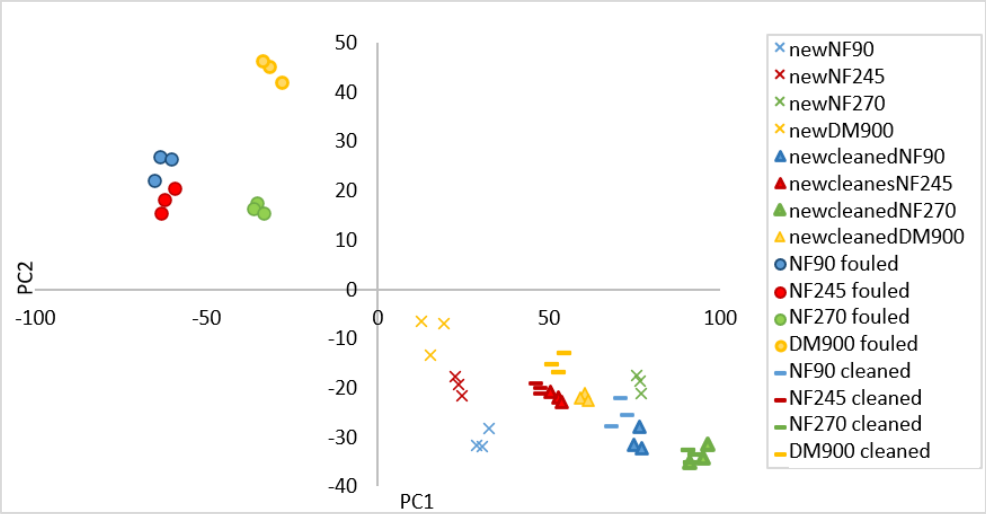

Fig. 12 Principal components (PCA) PC1 (71.24%var) and PC2 (16.41%var) of 2D fluorescence data for the nanofiltration tests with the model solution and after chemical cleaning. Operating conditions of nanofiltration test, 3 hours at CFV of 1 ms^{-1} and TMP of 10 bar

[colour figure]

In Fig. 13 the spectra of the NF270 membrane after the tests performed with MS and OMW are compared. It can be seen that the membrane fouled with OMW shows a greater signal reduction than the one fouled with MS. In the same way, both managed to recover the characteristic Ex/Em

signal after cleaning, but, as mentioned above, the signal was closer to that of a new membrane after cleaning than to that of the pristine membrane.

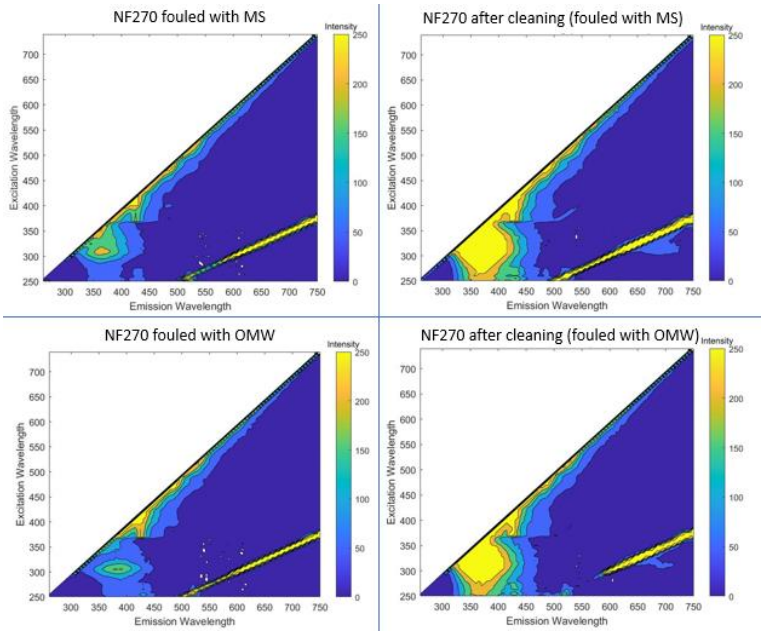

Fig. 13 2D fluorescence data of the NF270 membrane after nanofiltration tests with the model solution (MS) and olive mill wastewater (OMW). Operating conditions, 3 hours at CFV of 1 ms^{-1} and TMP of 10 bar.

[colour figure]

Fig. 14 shows the FTIR results for the tests performed with the NF270 membrane. The great difference between the new membrane and the membrane after cleaning is clearly seen. The large peak at around 3300 cm^{-1} could be attributed to preservation compounds such as glycerol [63]. On the other hand, the elimination of this peak for the membranes fouled by OMW and MS is associated with the adsorption of the phenolic compounds present in the samples [78]. Both membranes, fouled with MS and OMW, have lower signals at 1637.7 cm^{-1} and 900-1200 cm^{-1} than the pristine one, as HT and SUG were shown (Fig. 10) to attenuate these regions. However, the stronger effect was observed for the membrane fouled with OMW, which can be due to the adsorption of other compounds, such as proteins (at 1637.7 cm^{-1}) [79], polysaccharides and nucleic acids (at 900-1200 cm^{-1}) [80].

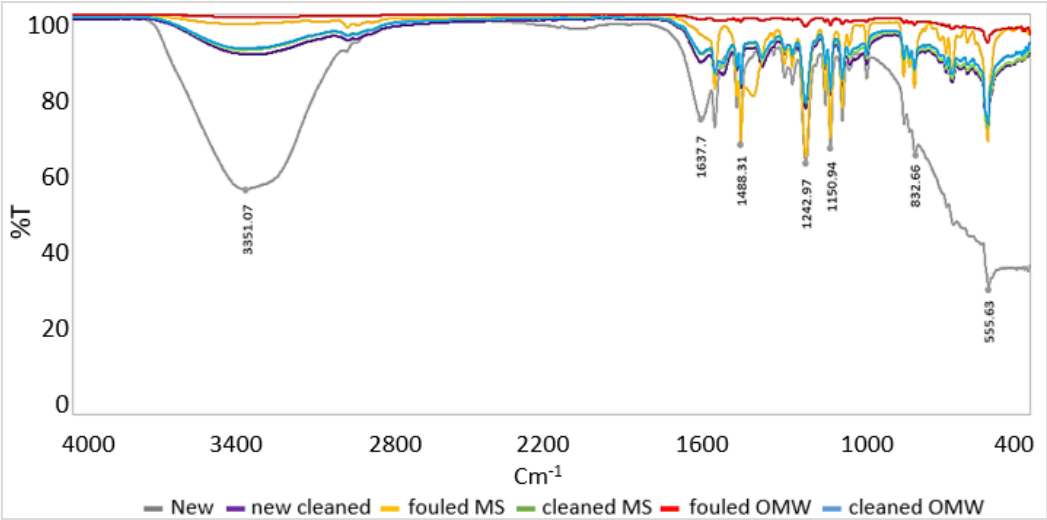

Fig. 14 FTIR spectra for the new and cleaned NF270 membrane and after the tests performed with the model solution (MS) and olive mill wastewater (OMW). Operating conditions, 3 hours at CFV of 1 ms^{-1} and TMP of 10 bar

[colour figure]

Finally, after cleaning the membranes fouled with MS and OMW, the spectra obtained were found to be similar to that observed for the new membrane after cleaning. For a better evaluation of the results, it was decided to perform the PCA analysis (Fig. 15). The PCA was used to compare the performance of the cleaning protocol, as well as to evaluate the similarity between the MS and the OMW. It can be seen in Fig. 15 that both membranes, fouled with MS and OMW, are close to each other, which implies a similarity between them. These results are inverse to those obtained after chemical cleaning, which are similar to those for the new cleaned membranes. It can be observed that the membrane fouled by the MS achieved a greater proximity to the new membrane after cleaning, which infers a greater cleaning efficiency. The differences between the membranes used with MS and OMW are probably due to the larger number of foulants present in the OMW, which led to higher fouling, making cleaning more difficult. Nevertheless, both membranes achieved optimal cleaning after undergoing the optimized cleaning protocol.

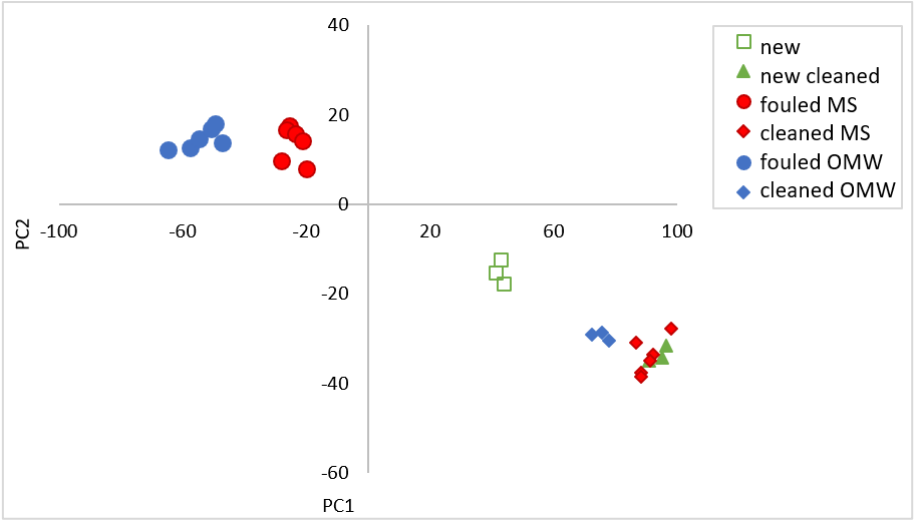

Fig. 15 PCA of 2D fluorescence data (62.52% and 14.89% of PC1 and PC2 variance, respectively) for the new and cleaned NF270 membrane and after the test with the model solution (MS) and olive mill wastewater (OMW). Operating conditions, 3 hours at CFV of 1 ms^{-1} and TMP of 10 bar

[colour figure]

Both feeds (MS and OOWW), as well as permeates and concentrates, were also analysed by 2D fluorescence spectroscopy. Through PCA (supplementary material, Fig S.3), a similarity between the two feed samples was observed, which implies that the fluorescence of the MS is representative of the real OMW. On the other hand, the quality of the permeates obtained was also verified, being similar after 5 and 180 minutes of operation for both types of feed streams.

4. Conclusions

Nanofiltration was studied as a possible second stage for an olive mill wastewater treatment, after a previous ultrafiltration step. Within the operating condition tested, the permeate flux was found to be more affected by transmembrane pressure than by crossflow velocity. All membranes were capable of concentrating phenolic compounds with a rejection greater than 70%. The membrane with the lowest molecular weight cut-off was the one that presented the highest percentage of rejection, but it did not achieve the established recovery (95%) of hydraulic permeability through the proposed cleaning protocols. The NF270 membrane under a cross flow velocity of 1 ms^{-1} and a transmembrane pressure of 10 bar was found to be the most suitable. After the analysis of different membranes and operating conditions, the effectiveness of nanofiltration to concentrate polyphenols from olive oil washing wastewaters, as well as to obtain a permeate suitable for reuse, was demonstrated.

Additionally, a study employing 2D Fluorescence and FTIR spectroscopy allowed to obtain valuable information about membrane fouling. Fluorescence analysis presented a more pronounced response to coloured compounds, while by means of FTIR it is possible to see more clearly the effect of the other tested foulant compounds. The main advantage of 2D Fluorescence spectroscopy is the possibility to use it for *in-situ* monitoring. According to both analyses, all tested compounds have an effect on the membrane surfaces. These techniques together represent a promising approach to analyse the efficiency of cleaning protocols.

Acknowledgements

The authors acknowledge the financial support of the Ministry of Economy, Industry and Competitiveness of Spain through the project CTM2017-88645-R, the European Union through the Operational Program of the Social Fund (FSE) financing ACIF-2018 and BEFPI-2021, and the Associate Laboratory for Green Chemistry-LAQV which is financed by national funds from FCT/MCTES (UIDB/50006/2020 and UIDP/50006/2020).

References

[1] J.M. Ochando-Pulido, A review on the use of membrane technology and fouling control for olive mill wastewater treatment, Sci. Total Environ. 563–564 (2016) 664–675. https://doi.org/10.1016/j.scitotenv.2015.09.151.

[2] E.O. Ezugbe, S. Rathilal, Membrane technologies in wastewater treatment: A review, Membranes (Basel). 10 (2020). https://doi.org/10.3390/membranes10050089.

[3] E. Kavitha, E. Poonguzhali, D. Nanditha, A. Kapoor, G. Arthanareeswaran, S. Prabhakar, Current status and future prospects of membrane separation processes for value recovery from wastewater, Chemosphere. 291 (2022) 132690. https://doi.org/https://doi.org/10.1016/j.chemosphere.2021.132690.

[4] N.N.R. Ahmad, W.L. Ang, Y.H. Teow, A.W. Mohammad, N. Hilal, Nanofiltration membrane processes for water recycling, reuse and product recovery within various industries: A review, J. Water Process Eng. 45 (2022) 102478. https://doi.org/10.1016/j.jwpe.2021.102478.

[5] Z. Su, T. Liu, X. Li, N.J.D. Graham, W. Yu, Tracking metal ion-induced organic membrane fouling in nanofiltration by adopting spectroscopic methods: Observations and predictions, Sci. Total Environ. 708 (2020) 135051. https://doi.org/10.1016/j.scitotenv.2019.135051.

[6] H.-P. Ma, H.-L. Wang, Y.-H. Qi, Z.-L. Chao, L. Tian, W. Yuan, L. Dai, W.-J. Lv, Reducing fouling of an industrial multi-stage nanofiltration membrane based on process

control: A novel shutdown system, J. Memb. Sci. 644 (2022) 120141. https://doi.org/10.1016/j.memsci.2021.120141.

[7] S. Zainith, L.F.R. Ferreira, G.D. Saratale, S.I. Mulla, R.N. Bharagava, Membrane-based hybrid processes in industrial waste effluent treatment, INC, 2021. https://doi.org/10.1016/B978-0-12-823804-2.00008-2.

[8] R. Castro-Muñoz, J. Yáñez-Fernández, V. Fíla, Phenolic compounds recovered from agro-food by-products using membrane technologies: An overview, Food Chem. 213 (2016) 753–762. https://doi.org/10.1016/j.foodchem.2016.07.030.

[9] B.M. Esteves, R. Fernandes, S. Morales-Torres, F.J. Maldonado–Hódar, A.M.T. Silva, L.M. Madeira, Integration of catalytic wet peroxidation and membrane distillation processes for olive mill wastewater treatment and water recovery, Chem. Eng. J. 448 (2022). https://doi.org/10.1016/j.cej.2022.137586.

[10] C.A. Paraskeva, V.G. Papadakis, E. Tsarouchi, D.G. Kanellopoulou, P.G. Koutsoukos, Membrane processing for olive mill wastewater fractionation, Desalination. 213 (2007) 218–229. https://doi.org/10.1016/j.desal.2006.04.087.

[11] T. Coskun, E. Debik, N.M. Demir, Treatment of olive mill wastewaters by nanofiltration and reverse osmosis membranes, Desalination. 259 (2010) 65–70. https://doi.org/10.1016/j.desal.2010.04.034.

[12] S. Sanches, M.C. Fraga, N.A. Silva, P. Nunes, J. Crespo, V.J. Pereira, Pilot scale nanofiltration treatment of olive mill wastewater: a technical and economical evaluation, Environ. Sci. Pollut. Res. 24 (2017) 3506–3518. https://doi.org/10.1007/s11356-016-8083-1.

[13] M. Cifuentes-Cabezas, C. Carbonell-Alcaina, M.C. Vincent-Vela, J.A. Mendoza-Roca, S. Álvarez-Blanco, Comparison of different ultrafiltration membranes as first step for the recovery of phenolic compounds from olive-oil washing wastewater, Process Saf. Environ. Prot. 149 (2021) 724–734. https://doi.org/10.1016/j.psep.2021.03.035.

[14] P. Tapia-Quirós, M.F. Montenegro-Landívar, M. Reig, X. Vecino, J. Saurina, M. Granados, J.L. Cortina, Integration of membrane processes for the recovery and separation of polyphenols from winery and olive mill wastes using green solvent-based processing, J. Environ. Manage. 307 (2022). https://doi.org/10.1016/j.jenvman.2022.114555.

[15] F. Di Caprio, L. Tayou Nguemna, M. Stoller, M. Giona, F. Pagnanelli, Microalgae cultivation by uncoupled nutrient supply in sequencing batch reactor (SBR) integrated with olive mill wastewater treatment, Chem. Eng. J. 410 (2021) 128417. https://doi.org/10.1016/j.cej.2021.128417.

[16] M. Kamali, D.P. Suhas, M.E. Costa, I. Capela, T.M. Aminabhavi, Sustainability considerations in membrane-based technologies for industrial effluents treatment, Chem.

Eng. J. 368 (2019) 474–494. https://doi.org/10.1016/j.cej.2019.02.075.

[17] H. Li, V. Chen, Chapter 10. Membrane Fouling and Cleaning in Food and Bioprocessing, Membr. Technol. (2010) 213–254. https://doi.org/10.1016/B978-1-85617-632-3.00010-0.

[18] W. Chen, C. Qian, K.G. Zhou, H.Q. Yu, Molecular Spectroscopic Characterization of Membrane Fouling: A Critical Review, Chem. 4 (2018) 1492–1509. https://doi.org/10.1016/j.chempr.2018.03.011.

[19] G. Rudolph, T. Virtanen, M. Ferrando, C. Güell, F. Lipnizki, M. Kallioinen, A review of in situ real-time monitoring techniques for membrane fouling in the biotechnology, biorefinery and food sectors, J. Memb. Sci. 588 (2019) 117221. https://doi.org/10.1016/j.memsci.2019.117221.

[20] O. Abbas, A. Pissard, V. Baeten, 3 - Near-infrared, mid-infrared, and Raman spectroscopy, Second Edi, Elsevier Inc., 2020. https://doi.org/10.1016/B978-0-12-813266-1/00003-6.

[21] S. Pawlowski, C.F. Galinha, J.G. Crespo, S. Velizarov, 2D fluorescence spectroscopy for monitoring ion-exchange membrane based technologies - Reverse electrodialysis (RED), Water Res. 88 (2016) 184–198. https://doi.org/10.1016/j.watres.2015.10.010.

[22] C.F. Galinha, G. Carvalho, C.A.M. Portugal, G. Guglielmi, M.A.M. Reis, J.G. Crespo, Multivariate statistically-based modelling of a membrane bioreactor for wastewater treatment using 2D fluorescence monitoring data, Water Res. 46 (2012) 3623–3636. https://doi.org/10.1016/j.watres.2012.04.010.

[23] L. Lenhardt, R. Bro, I. Zeković, T. Dramićanin, M.D. Dramićanin, Fluorescence spectroscopy coupled with PARAFAC and PLS DA for characterization and classification of honey, Food Chem. 175 (2015) 284–291. https://doi.org/10.1016/j.foodchem.2014.11.162.

[24] M. Cabrera-Bañegil, M. del C. Hurtado-Sánchez, T. Galeano-Díaz, I. Durán-Merás, Front-face fluorescence spectroscopy combined with second-order multivariate algorithms for the quantification of polyphenols in red wine samples, Food Chem. 220 (2017) 168–176. https://doi.org/10.1016/j.foodchem.2016.09.152.

[25] L. Benavente, C. Coetsier, A. Venault, Y. Chang, C. Causserand, P. Bacchin, P. Aimar, FTIR mapping as a simple and powerful approach to study membrane coating and fouling, J. Memb. Sci. 520 (2016) 477–489. https://doi.org/10.1016/j.memsci.2016.07.061.

[26] M.N. Pons, S. Le Bonté, O. Potier, Spectral analysis and fingerprinting for biomedia characterisation, J. Biotechnol. 113 (2004) 211–230. https://doi.org/10.1016/j.jbiotec.2004.03.028.

[27] Z. Chen, J. Luo, X. Hang, Y. Wan, Physicochemical characterization of tight

nanofiltration membranes for dairy wastewater treatment, J. Memb. Sci. 547 (2018) 51–63. https://doi.org/10.1016/j.memsci.2017.10.037.

[28] C.M. Sánchez-Arévalo, Á. Jimeno-Jiménez, C. Carbonell-Alcaina, M.C. Vincent-Vela, S. Álvarez-Blanco, Effect of the operating conditions on a nanofiltration process to separate low-molecular-weight phenolic compounds from the sugars present in olive mill wastewaters, Process Saf. Environ. Prot. 148 (2021) 428–436. https://doi.org/10.1016/j.psep.2020.10.002.

[29] A. Volkov, Membrane Compaction, in: E. Drioli, L. Giorno (Eds.), Encycl. Membr., Springer, Berlin, Heidelberg, 2014. https://doi.org/10.1007/978-3-642-40872- 4_1404-2.

[30] N. Tanne, R. Xu, M. Zhou, P. Zhang, X. Wang, X. Wen, Influence of pore size and membrane surface properties onarsenic removal by nanofiltration membranes, Front. Environ. Sci. Eng. Vol. 13 (2019) 19. https://doi.org/10.1007/s11783-019-1105-8.

[31] Y. Suo, Y. Ren, Research on the mechanism of nanofiltration membrane fouling in zero discharge process of high salty wastewater from coal chemical industry, Chem. Eng. Sci. 245 (2021) 116810. https://doi.org/10.1016/j.ces.2021.116810.

[32] C.P. Leo, M.Z. Yahya, S.N.M. Kamal, A.L. Ahmad, A.W. Mohammad, Potential of nanofiltration and low pressure reverse osmosis in the removal of phosphorus for aquaculture, Water Sci. Technol. 67 (2013) 831–837. https://doi.org/10.2166/wst.2012.625.

[33] L. Gao, H. Wang, Y. Zhang, M. Wang, Nanofiltration membrane characterization and application: Extracting lithium in lepidolite leaching solution, Membranes (Basel). 10 (2020) 1–18. https://doi.org/10.3390/membranes10080178.

[34] U.T. Syed, C. Brazinha, J.G. Crespo, J.M. Ricardo-da-Silva, Valorisation of grape pomace: Fractionation of bioactive flavan-3-ols by membrane processing, Sep. Purif. Technol. 172 (2017) 404–414. https://doi.org/10.1016/j.seppur.2016.07.039.

[35] M.J. López-Muñoz, A. Sotto, J.M. Arsuaga, B. Van der Bruggen, Influence of membrane, solute and solution properties on the retention of phenolic compounds in aqueous solution by nanofiltration membranes, Sep. Purif. Technol. 66 (2009) 194–201. https://doi.org/10.1016/j.seppur.2008.11.001.

[36] A. Santafé-Moros, J.M. Gonzálvez-Zafrilla, D. Valencia, Design of a Flat Membrane Module for Fouling and Permselectivity Studies, in: COMSOL Conf. Paris, 2010. http://www.comsol.asia/papers/8300/download/gozalvez-zafrilla_paper.pdf.

[37] APHA, Standard Methods for the Examination of Water and Wastewater, in: Am. Public Heal. Assoc. Washington, DC, 2005: p. 21 st. ed.

[38] V.L. Singleton, R. Orthofer, R.M. Lamuela-Raventós, Analysis of total phenols and other oxidation substrates and antioxidants by means of folin-ciocalteu reagent, Methods Enzymol. 299 (1999) 152–178. https://doi.org/10.1016/S0076-6879(99)99017-1.

[39] B. Frolund, P. Rikke, K. Keiding, P.H. Nielsen, Extraction of extracellular polymers from activated sludge using a cation exchange resin, Water Res. 30 (1996) 1749–1758.

[40] M. Cifuentes-Cabezas, C.M. Sanchez-Arévalo, J.A. Mendoza-Roca, M.C. Vincent-Vela, S. Álvarez-Blanco, Recovery of Phenolic Compounds from Olive Oil Washing Wastewater by Adsorption/Desorption Process, Sep. Purif. Technol. 298 (2022) 121562. https://doi.org/10.1016/j.seppur.2022.121562.

[41] A.M. Avram, P. Morin, C. Brownmiller, L.R. Howard, A. Sengupta, S.R. Wickramasinghe, Concentrations of polyphenols from blueberry pomace extract using nanofiltration, Food Bioprod. Process. 106 (2017) 91–101. https://doi.org/10.1016/j.fbp.2017.07.006.

[42] J.A. Arboleda Mejia, A. Ricci, A.S. Figueiredo, A. Versari, A. Cassano, G.P. Parpinello, M.N. de Pinho, Recovery of phenolic compounds from red grape pomace extract through nanofiltration membranes, Foods. 9 (2020). https://doi.org/10.3390/foods9111649.

[43] P. Bacchin, P. Aimar, R.W. Field, Critical and sustainable fluxes: Theory, experiments and applications, J. Memb. Sci. 281 (2006) 42–69. https://doi.org/10.1016/j.memsci.2006.04.014.

[44] A.I. Schäfer, A.G. Fane, T.D. Waite, Nanofiltration of natural organic matter: Removal, fouling and the influence of multivalent ions, Desalination. 118 (1998) 191–204.

[45] M. Mänttäri, M. Nyström, Critical flux in NF of high molar mass polysaccharides and effluents from the paper industry, J. Memb. Sci. 170 (2000) 257–273. https://doi.org/10.1016/S0376-7388(99)00373-7.

[46] A.W. Mohammad, Y.H. Teow, W.L. Ang, Y.T. Chung, D.L. Oatley-Radcliffe, N. Hilal, Nanofiltration membranes review: Recent advances and future prospects, Desalination. 356 (2015) 226–254. https://doi.org/10.1016/j.desal.2014.10.043.

[47] M.A. Nunes, S. Pawlowski, A.S.G. Costa, R.C. Alves, M.B.P.P. Oliveira, S. Velizarov, Valorization of olive pomace by a green integrated approach applying sustainable extraction and membrane-assisted concentration, Sci. Total Environ. 652 (2019) 40–47. https://doi.org/10.1016/j.scitotenv.2018.10.204.

[48] A. Böcking, Membrane Transport Properties and Process Design in Nanofiltration with Organic Solvents and Aqueous Solvent Mixtures, 2020.

[49] A.R. Costa, M.N. De Pinho, Effect of membrane pore size and solution chemistry on the ultrafiltration of humic substances solutions, J. Memb. Sci. 255 (2005) 49–56. https://doi.org/10.1016/j.memsci.2005.01.016.

[50] G.S. Vieira, F.K.V. Moreira, R.L.S. Matsumoto, M. Michelon, F.M. Filho, M.D. Hubinger, Influence of nanofiltration membrane features on enrichment of jussara ethanolic extract (Euterpe edulis) in anthocyanins, J. Food Eng. (2018). https://doi.org/10.1016/j.jfoodeng.2018.01.013.

[51] A. Giacobbo, A.M. Bernardes, M.N. de Pinho, Sequential pressure-driven membrane operations to recover and fractionate polyphenols and polysaccharides from second racking wine lees, Sep. Purif. Technol. 173 (2017) 49–54. https://doi.org/10.1016/j.seppur.2016.09.007.

[52] J. Geens, K. Peeters, B. Van Der Bruggen, C. Vandecasteele, Polymeric nanofiltration of binary water-alcohol mixtures: Influence of feed composition and membrane properties on permeability and rejection, J. Memb. Sci. 255 (2005) 255–264. https://doi.org/10.1016/j.memsci.2005.01.039.

[53] A. López-borrell, M.F. López-Pérez, S.C. Cardona, J. Lora-garcía, Experimental Study and Mathematical Modeling of a Nanofiltration Membrane System for the Recovery of Polyphenols from Wine Lees, Membranes (Basel). 12 (2022) 240. https://doi.org/10.3390/membranes12020240.

[54] N. Nguyen, C. Fargues, W. Guiga, M.L. Lameloise, Assessing nanofiltration and reverse osmosis for the detoxification of lignocellulosic hydrolysates, J. Memb. Sci. 487 (2015) 40–50. https://doi.org/10.1016/j.memsci.2015.03.072.

[55] M. Mänttäri, A. Pihlajamäki, M. Nyström, Effect of pH on hydrophilicity and charge and their effect on the filtration efficiency of NF membranes at different pH, J. Memb. Sci. 280 (2006) 311–320. https://doi.org/10.1016/j.memsci.2006.01.034.

[56] M. Bédas, G. Tanguy, A. Dolivet, S. Méjean, F. Gaucheron, G. Garric, G. Senard, R. Jeantet, P. Schuck, Nanofiltration of lactic acid whey prior to spray drying: Scaling up to a semi-industrial scale, LWT - Food Sci. Technol. 79 (2017) 355–360. https://doi.org/10.1016/j.lwt.2017.01.061.

[57] C.P. Leo, W.K. Chai, A.W. Mohammad, Y. Qi, A.F.A. Hoedley, S.P. Chai, Phosphorus removal using nanofiltration membranes, Water Sci. Technol. 64 (2011) 199–205. https://doi.org/10.2166/wst.2011.598.

[58] N. Nguyen, C. Fargues, R. Lewandowski, W. Guiga, M.L. Lameloise, Assessing nanofiltration and reverse osmosis for the detoxification of fermentable solutions, Procedia Eng. 44 (2012) 1476–1478. https://doi.org/10.1016/j.proeng.2012.08.834.

[59] J.M. Ochando-Pulido, J.R. Corpas-Martínez, A. Martinez-Ferez, About two-phase olive oil washing wastewater simultaneous phenols recovery and treatment by nanofiltration, Process Saf. Environ. Prot. 114 (2018) 159–168. https://doi.org/10.1016/j.psep.2017.12.005.

[60] M.C. Martí-Calatayud, S. Schneider, M. Wessling, On the rejection and reversibility of fouling in ultrafiltration as assessed by hydraulic impedance spectroscopy, J. Memb. Sci. 564 (2018) 532–542. https://doi.org/10.1016/j.memsci.2018.07.021.

[61] R.W. Field, G.K. Pearce, Critical, sustainable and threshold fluxes for membrane filtration with water industry applications, Adv. Colloid Interface Sci. 164 (2011) 38–44.

https://doi.org/10.1016/j.cis.2010.12.008.

[62] B. Van der Bruggen, M. Mänttäri, M. Nyström, Drawbacks of applying nanofiltration and how to avoid them: A review, Sep. Purif. Technol. 63 (2008) 251–263. https://doi.org/10.1016/j.seppur.2008.05.010.

[63] M. Gryta, J. Bastrzyk, D. Lech, Evaluation of fouling potential of nanofiltration membranes based on the dynamic contact angle measurements, Polish J. Chem. Technol. 14 (2012) 97–104. https://doi.org/10.2478/v10026-012-0091-4.

[64] A. Cassano, C. Conidi, R. Ruby-Figueroa, R. Castro-Muñoz, Nanofiltration and tight ultrafiltration membranes for the recovery of polyphenols from agro-food by-products, Int. J. Mol. Sci. 19 (2018) 351. https://doi.org/10.3390/ijms19020351.

[65] A. Cassano, W. Cabri, G. Mombelli, F. Peterlongo, L. Giorno, Recovery of bioactive compounds from artichoke brines by nanofiltration, Food Bioprod. Process. 98 (2016) 257–265. https://doi.org/10.1016/j.fbp.2016.02.004.

[66] T.M. Olajide, T. Liu, H. Liu, X. Weng, Antioxidant properties of two novel lipophilic derivatives of hydroxytyrosol, Food Chem. 315 (2020) 126197. https://doi.org/10.1016/j.foodchem.2020.126197.

[67] H. Fu, Y. Sun, H. Teng, D. Zhang, Z. Xiu, Salting-out extraction of carboxylic acids, Sep. Purif. Technol. 139 (2015) 36–42. https://doi.org/10.1016/j.seppur.2014.11.001.

[68] L. Quintieri, P. Palatini, A. Nassi, P. Ruzza, M. Floreani, Flavonoids diosmetin and luteolin inhibit midazolam metabolism by human liver microsomes and recombinant CYP 3A4 and CYP3A5 enzymes, Biochem. Pharmacol. 75 (2008) 1426–1437. https://doi.org/10.1016/j.bcp.2007.11.012.

[69] S. Son, B.A. Lewis, Free radical scavenging and antioxidative activity of caffeic acid amide and ester analogues: Structure-activity relationship, J. Agric. Food Chem. 50 (2002) 468–472. https://doi.org/10.1021/jf010830b.

[70] J.F. Fernández, B. Jastorff, R. Störmann, S. Stolte, J. Thöming, Thinking in terms of structure-activity-relationships (T-SAR): A tool to better understand nanofiltration membranes, Membranes (Basel). 1 (2011) 162–183. https://doi.org/10.3390/membranes1030162.

[71] M.-J. Corbatón-Báguena, S. Álvarez-blanco, M.C. Vincent-Vela, Cleaning of ultrafiltration membranes fouled with BSA by means of saline solutions, Sep. Purif. Technol. 125 (2014) 1–10. https://doi.org/10.1016/j.seppur.2014.01.035.

[72] M. Gryta, Resistance of polypropylene membrane to oil fouling during membrane distillation, Membranes (Basel). 11 (2021). https://doi.org/10.3390/membranes11080552.

[73] H. Siddique, E. Rundquist, Y. Bhole, L.G. Peeva, A.G. Livingston, Mixed matrix membranes for organic solvent nanofiltration, J. Memb. Sci. 452 (2014) 354–366.

https://doi.org/10.1016/j.memsci.2013.10.012.

[74] C.F. Galinha, G. Carvalho, C.A.M. Portugal, G. Guglielmi, M.A.M. Reis, J.G. Crespo, Two-dimensional fluorescence as a fingerprinting tool for monitoring wastewater treatment systems, J. Chem. Technol. Biotechnol. 86 (2011) 985–992. https://doi.org/10.1002/jctb.2613.

[75] M. Sá, J. Monte, C. Brazinha, C.F. Galinha, J.G. Crespo, 2D Fluorescence spectroscopy for monitoring Dunaliella salina concentration and integrity during membrane harvesting, Algal Res. 24 (2017) 325–332. https://doi.org/10.1016/j.algal.2017.04.013.

[76] S. Pawlowski, C.F. Galinha, J.G. Crespo, S. Velizarov, Prediction of reverse electrodialysis performance by inclusion of 2D fluorescence spectroscopy data into multivariate statistical models, Sep. Purif. Technol. 150 (2015) 159–169. https://doi.org/10.1016/j.seppur.2015.06.032.

[77] A. Simon, W.E. Price, L.D. Nghiem, Effects of chemical cleaning on the nanofiltration of pharmaceutically active compounds (PhACs), Sep. Purif. Technol. 88 (2012) 208–215. https://doi.org/10.1016/j.seppur.2011.12.009.

[78] B.H. Gursoy-Haksevenler, I. Arslan-Alaton, UV fluorescence, FTIR, and GC–MS analyses and resin fractionation procedures as indicators of the chemical treatability of olive mill wastewater, Desalin. Water Treat. 57 (2016) 2372–2382. https://doi.org/10.1080/19443994.2014.992979.

[79] J. Bastrzyk, M. Gryta, K. Karakulski, Fouling of nanofiltration membranes used for separation of fermented glycerol solutions, Chem. Pap. 68 (2014) 757–765. https://doi.org/10.2478/s11696-013-0520-8.

[80] A. Houari, D. Seyer, K. Kecili, V. Heim, P. Di Martino, Kinetic development of biofilm on NF membranes at the Méry-sur-Oise plant, France, Biofouling. 29 (2013) 109–118. https://doi.org/10.1080/08927014.2012.752464.